Seeing through scattering media with time-reversed light

Mooseok Jang, Haowen Ruan, Haojiang (Edward) Zhou, Ying Min Wang, Benjamin Judkewitz, Daifa Wang and Changhuei Yang

Biophotonics Laboratory, California Institute of Technology

Abstract

Optical turbidity of biological tissues poses a big challenge in light focusing and imaging deep inside the tissue. Optical phase conjugation (OPC) technique is the technique that can be exploited to time-reverse the light through the turbid media. The time-reversed light cancel out the wavefront distortion from multiple scattering and traces back the original light due to the time reversal symmetry of scattering event. This effectively enables us to see through the scattering media. A variety of OPC-based techniques were demonstrated to image and focus light through or inside the scattering media.

Turbidity suppression by digital optical phase conjugation (DOPC)

A challenge for biomedical applications of analog OPC is that the conventional nonlinear optics based methods provide fairly limited OPC reflectivity. Inspired by acoustic time reversal techniques, we have developed a digital OPC method (DOPC) that can in principle provide unlimited OPC reflectivity.

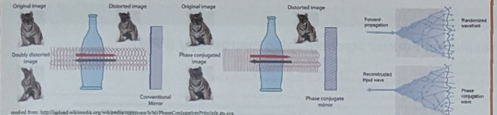

modified from: http://upload.wikimedia.org/wikipedia/commons/b/b0/PhaseConjugationPrinciple.ps.svg

Conventional mirror versus phase conjugate mirror

Forward and time reversed wavefront. Elastic light scattering is the dominant process through which wavefront is randomized. Phase conjugation can effectively time reverse the scattering process and undo the distortion.

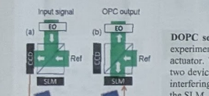

DOPC setup (left). The design of DOPC is inspired by the time reversal experiment, in which a sound transducer is used both as a sensor and an actuator. We optically combine the SLM with a CCD camera such that the two devices form virtual images. The wavefront is recorded by CCD through interfering the transmission with a reference light field, and played back by the SLM.

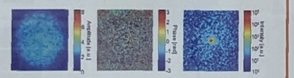

DOPC results (right). Measured amplitude and phase profile of the incident wave, and the reconstructed beam profile.

- Conventional focusing methods treat scattered light as noise and select for ballistic light, which exponentially decreases with depth.
- Scattering is a deterministic process and is reversible through optical phase conjugation (OPC).
- We can effectively time reverse the scattering process and undo the distortion caused by scattering.

Auto-alignment of DOPC systems based on digital propagation

Here, we present a method for auto-alignment of a DOPC system by which the misalignment between the sensor and the SLM is auto-corrected through digital light propagation. With this method, we were able to accomplish OPC playback with a DOPC system with gross sensor-SLM misalignment by an axial displacement of up to 1.5 cm , rotation and tip/tilt of 5°, and in-plane displacement of .5 mm (dependent on the physical size of the sensor and the SLM). Our auto-alignment method robustly achieved a DOPC playback peak-to-background ratio (PBR) corresponding to more than ~30% of the theoretical maximum.

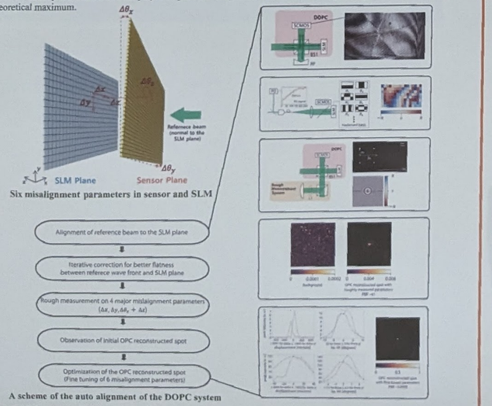

Six misalignment parameters in sensor and SLM

A scheme of the auto alignment of the DOPC system

- DOPC system, which conventionally requires one-to-one pixel match of sensor and SLM pixel, can now be virtually aligned in an automated manner using digital light propagation technique.
- DOPC system can be easily recovered from the day-to-day misalignment (mechanical shock, thermal drift, etc.) .

Optical phase conjugation (OPC)-assisted isotropic focusing

Here, we present an optical phase conjugation (OPC)-assisted isotropic focusing method. We exploit the time-reversal nature of OPC playback to naturally guarantee the overlap of the two focused beams even when the objective lenses are significantly misaligned (up to 140 microns transversely and 80 microns axially demonstrated). The scattering correction capability of OPC also enabled us to accomplish isotropic focusing through thick scattering samples (demonstrated with samples of ~7 scattering mean free paths).

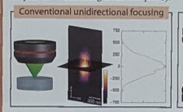

Conventional unidirectional focusing and isotropic focusing (left). Axial spot size is 3-5 times reduced with the isotropic focusing. However, the exacting requirement on the alignment – overlap of two foci – and its intolerance to the sample turbidity have significantly limited its utility.

Conventional isotropic focusing and OPC-assisted isotropic focusing (right). The original beam (coming from the top) creates a sharp focus, propagates through sample and the objective lens at the bottom. DOPC system is placed under the objective lens at the bottom. **(a, DOPC OFF)** When DOPC is off, the system performs as the conventional isotropic focusing system and the objective lens at the bottom creates the focus independently. **(b, DOPC ON)** When DOPC is on, the objective lens at the bottom (OPC-assisted) creates the focus overlapped with the focus created by the objective lens on the top. **(c)** Measured OPC phase map of the wavefront exiting the objective lens at the bottom.

1 : laterally misaligned objectives
2 : axially misaligned objectives
3 : optically inhomogeneous sample

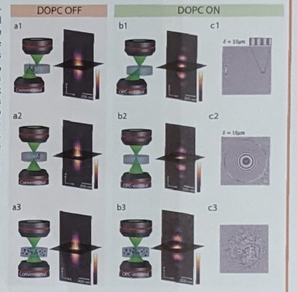

- Time reversal characteristic of optical phase conjugation naturally guarantees the overlap of two foci from two objectives so that it resolves two big challenges in the conventional isotropic focusing technique.
- This method can potentially improve 4Pi microscopy and 3D microstructure patterning.

Light focusing on the moving target

Optical time reversal focusing can be achieved by using a moving object as a novel guide star. By differentiating time-varying scattering fields caused by a moving object and applying optical time-reversal, light can be focused back to the location previously occupied by the object. We further demonstrate that the generated focus can be used to noninvasively count particles in a flow-cytometry configuration – even when the particles are hidden behind a strong diffusor. By achieving optical time-reversal and focusing noninvasively without any external guide-stars (using just intrinsic characteristics of the sample), this work paves the way to a range of scattering media imaging applications including underwater and atmospheric focusing as well as noninvasive *in vivo* flow-cytometry.

Focusing on a moving target in a scattering sample (right) (a) Target at position 1 (far off the illuminated field-of-view); **(b)** Target at position 2 (within the illuminated field-of-view); **(c)** focusing result behind diffusor; **(d-f)** Cross section intensity distribution, which indicates a PBR over 500 (scale bars in a, b and c are 100 μm); **(g)** scattering field phase map on SLM when target is at position 1; **(h)** scattering field phase map on SLM when target is at position 2; **(i)** phase map of differentiated fields (scale bars in e, f and g all stand for 1 mm).

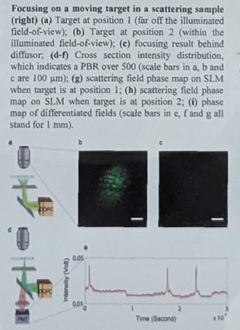

Optical flow cytometry in scattering media (left) (a) Laser speckle shining on the microfluidic channel; **(b)** bright field image of the guide star bead in the microfluidic channel; **(c)** conjugate focusing at the corresponding position in the microfluidic channel; **(d-e)** Cytometry signal captured on the PMT when fluorescence beads flowed by.

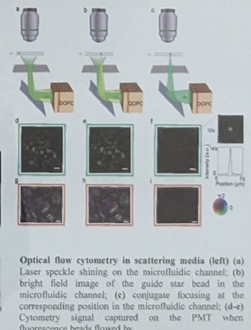

- Moving target such as bead and blood cell is used as an guide star.
- Taking the difference of two optical field with target at different positions, we are able to focus light back to the original position of the target by DOPC.
- The focused light beam can be used as a probe for optical flow cytometry.

Time reversed ultrasonically encoded (TRUE) light focusing

In order to create a 'free moving' guide star *inside* scattering media, focused ultrasound pulses were used as a virtual guide star. Using digital time reversal of ultrasound-encoded light, we directly demonstrate focusing and fluorescence imaging deep inside biological tissues. We further illustrate the potential of our method for fluorescence bioimaging in the diffusive regime by imaging complex fluorescent objects and tumor microtissues 2.5 mm deep in biological tissues, at an anisotropic lateral resolution of 36 μm by 52 μm.

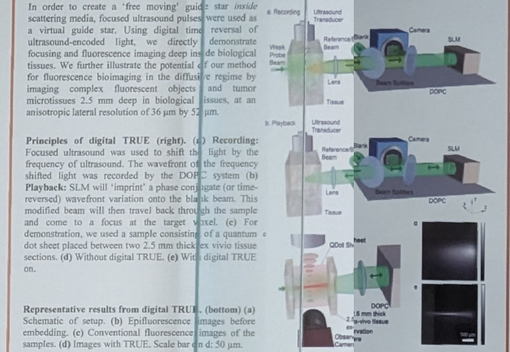

Principles of digital TRUE (right). (a) Recording: Focused ultrasound was used to shift the light by the frequency of ultrasound. The wavefront of the frequency shifted light was recorded by the DOPC system (b) **Playback:** SLM will 'imprint' a phase conjugate (or time-reversed) wavefront variation onto the back beam. This modified beam will then travel back through the sample and come to a focus at the target voxel. (c) For demonstration, we used a sample consisting of a quantum dot sheet placed between two 2.5 mm thick ex vivio tissue sections. **(d)** Without digital TRUE. **(e)** With digital TRUE on.

Representative results from digital TRUE. (bottom) (a) Schematic of setup. **(b)** Epifluorescence images before embedding. **(c)** Conventional fluorescence images of the samples. **(d)** Images with TRUE. Scale bar on d: 50 μm.

- Focused ultrasound pulse acts as a guide star.
- Wavefront of the frequency shifted light is recorded by digital holography method.
- Phase conjugated light travels back to the focus of the ultrasound.
- Size of the optical focal point depends on the size of the ultrasound focus.
- Penetration depth has been demonstrated to ~2.5 mm penetration with PBR at ~5.

Estimation on the penetration depth limit of the TRUE

This theoretical study aims to explore the depth limits of the TRUE technique for biological tissues in the context of two primary constraints – the safety limit of the incident light fluence and delimited TRUE's recording time (assumed to be 1 ms), as dynamic scatterer movements in a living sample can break the time-reversal symmetry. Our numerical simulation indicates that TRUE has the potential to render an optical focus with a peak-to-background ratio of ~2 at a depth of ~103 mm at wavelength of 800 nm in a phantom with tissue scattering characteristics.

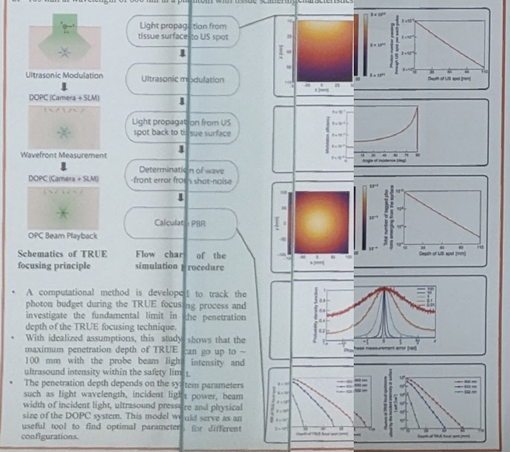

Schematics of TRUE focusing principle **Flow chart of the simulation procedure**

- A computational method is developed to track the photon budget during the TRUE focusing process and investigate the fundamental limit in the penetration depth of the TRUE focusing technique.
- With idealized assumptions, this study shows that the maximum penetration depth of TRUE can go up to ~ 100 mm with the probe beam light intensity and ultrasound intensity within the safety limit.
- The penetration depth depends on the system parameters such as light wavelength, incident light power, beam width of incident light, ultrasound pressure and physical size of the DOPC system. This model would serve as an useful tool to find optimal parameters for different configurations.

Iterative TRUE (iTRUE)

To improve the light intensity and resolution at the TRUE focus, we developed an iterative TRUE light focusing technique which employs the TRUE focal spot itself as a signal source (rather than the diffused light) for subsequent TRUE procedures. Importantly, this iTRUE technique allows light focusing in backscattering mode. We demonstrate that the intensity of the light focus is progressively enhanced by a factor of ~22 and the focusing resolution in the ultrasound axial and lateral directions is improved ~2-fold and ~3-fold respectively.

Principle of the iTRUE (right). (a) Schematic experimental setup **(b)** The probe beam diffuses inside the scattering sample when the SLM is initially uncontrolled. **(c)** With ultrasound modulation, a small fraction of the probe beam is shifted in frequency and backscattered to the DOPC system. **(d)** The phase-conjugated copy of the measured ultrasound modulated light is sent back to the sample and modulated simultaneously by the ultrasound. A more accurate wavefront can be measured for the next step. **(e)** A stronger light focus can thus be obtained.

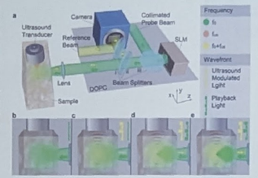

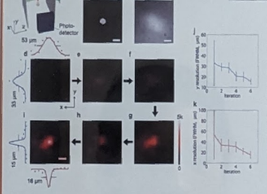

Image scanning of a fluorescent bead (left). (a) Experiment arrangement. The ultrasound focus scanned the sample on the x-y plane. The fluorescence intensity was measured at each iteration using the photodetector. **(b-c)** Microscopic images of the fluorescent bead without and with the scattering film. **(d-i)** Intensity map of the fluorescent signals (11x11 scanning points with cubic interpolation). **(j, k)** The resolution (FWHM of the Gaussian profile) in the y direction and the x direction of the fluorescent bead image over 6 iterations. Error bar indicates 95% confidence bound. All scale bars are 20 μm.

- Play back of the phase conjugated light and recording of the ultrasound modulated light wavefront occurs simultaneously.
- Light intensity enhancement by ~20 times at the ultrasound focus has been demonstrated.
- Image resolution can also be improved as ultrasound pressure profile can be approximated to be a Gaussian function.
- System works in both transmission and back scattering geometry.

Speckle-scale focusing with time reversal of variance-encoded light (TROVE)

In TRUE-imaging, the resolution is limited to the ultrasound focus. To break the barrier and reaching the theoretical resolution limit, we developed a new approach termed time-reversal of variance-encoded light.

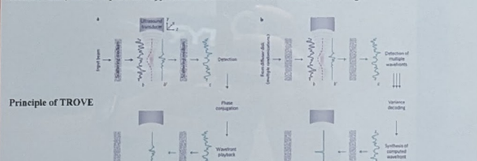

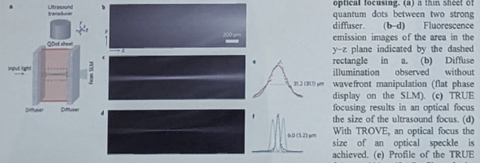

Visualization of speckle-scale optical focusing. (a) a thin sheet of quantum dots between two strong diffuser. **(b-d)** Fluorescence emission images of the area in the y-z plane indicated by the dashed rectangle in a. **(b)** Diffuse illumination observed without wavefront manipulation (flat phase display on the SLM). **(c)** TRUE focusing results in an optical focus the size of the ultrasound focus. **(d)** With TROVE, an optical focus the size of an optical speckle is achieved. **(e)** Profile of the TRUE focus width. **(f)** Profile of the TROVE focus .

Point-spread function and image acquisition. (a) Epifluorescence image of a single bead. **(b)** Epifluorescence image of a single bead as seen through a diffuser. **(c)** Fluorescence image of single bead obtained by raster-scanning a TRUE focus. **(d)** Fluorescence image of single bead obtained using TROVE.

Turbidity suppression through *in vivo* sample

In living tissue, scatterers are highly movable and the movement can break the time-reversal symmetry when there is a latency in the OPC playback. We investigated this decorrelation characteristic time through the 1.5 mm thick dorsal skin flap of a living mouse at different levels of immobilization.

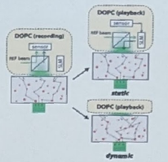

Digital optical phase conjugation (DOPC) process through moving scatterers.

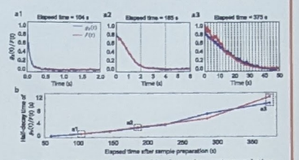

Simultaneously-measured speckle intensity autocorrelation function and OPC spot intensity through tissue phantom. For different time scales, two curves show close agreement in the time characteristic.

Mouse dorsal skin flap model. Mouse dorsal skin is pinched with two acrylic plates secured by four bolts and nuts.

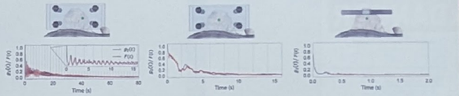

Speckle intensity autocorrelation function and turbidity suppression fidelity measured through mouse dorsal skin flap. Decorrelation characteristic significantly varied depending on the degree of immobilization. **(left)** When the skin was directly pinched, both profiles dropped to 0.5 in ~2 seconds. Considerable correlation between speckle (>0.1) patterns were observed till ~30 seconds. **(middle)** When the surrounding region was pinched, the characteristic time reduced to ~ 500 ms as the scatterers are less immobilized. **(right)** This further reduced down to ~50 ms for the intact skin. Intensity autocorrelation function and turbidity suppression fidelity oscillated in the frequency of breath. The speckle intensity autocorrelation function and OPC spot intensity observed good match in decorrelation characteristic.

- This study implies that the OPC spot can survive for an even lower speckle autocorrelation as long as the initial spot contrast is high enough, which can be simply achieved by increasing the number of controllable optical modes (pixel number) in the DOPC system.
- This opens up the new possibility of using the OPC process for turbidity suppression of biological tissue because the feasibility of the OPC system can even be extended into the regime where the scatterer dynamics are much faster than the OPC system speed.

Conclusions

- OPC process generates the time-reversed beam and, in turn, enables us to see through the turbid biological tissue.
- Digital version of OPC system provides in principle an infinite phase conjugation reflectivity, which is suitable for biomedical applications.
- Time-reversal characteristic of OPC beam naturally guarantees the generation of light standing-wave, which can be exploited for isotropic focusing.
- Moving targets can be exploited as a guide-star for OPC process, which is suitable for blood cell counting.
- Ultrasound-encoded light can be time-reversed to create focus light and image through or inside biological tissue.
- Iterative focusing and variance light encoding can be combined with TRUE technique to enhance the brightness and spatial resolution.
- Turbidity suppression fidelity through in-vivo tissue is confirmed with rabbit ear and mouse skin. Development in spatial light modulator and sensor technology will assure better fidelity.
- Our results set the stage for broad use of OPC in practical biomedical applications requiring optical interrogation in deep tissue such as imaging, photodynamic therapy, spectroscopy and neuron stimulation.

References

[1] Z. Yaqoob, D. Psaltis, M. S. Feld, and C. Yang, Nature Photonics 2, 110-115 (2008).
[2] I. M. Vellekoop, University of Twente Thesis, 1-142 (2008).
[4] E. J. McDowell, M. Cui, I. M. Vellekoop, V. Senekerimyan, Z. Yaqoob, and C. Yang. Journal of Biomedical Optics 15, 025004 (2010).
[5] M. Cui and C. Yang, Optics Express 18, 3444-3455 (2010).
[7] X. Xu, H. Liu, and L. V. Wang, Nature Photonics 5, 154-157 (2011).
[8] Y. M. Wang*, B. Judkewitz*, C. A. DiMarzio, and C. Yang, Nature Communication 3, 928 (2012).
[9] B. Judkewitz*, Y. M. Wang*, R. Horstmeyer, A. Mathy, and C. Yang, Nature Photonics 17, 300-305 (2013).
[10] M. Jang, H. Ruan, B. Judkewitz, and C. Yang, Optics Express 22, 5787-5807 (2014).
[11] M. Jang*, H. Ruan*, H. Zhou, B. Judkewitz, and C. Yang, Optics Express 22, 14054-71 (2014).

Acknowlegements

This work was supported by NIH 1DP2OD007307-01 & R21 EB012255, DARPA W31P4Q-11-1-0008.